Journal of Hydroscience and Hydraulic Engineering
Vol. 20, No.1 May, 2002, 137-150

A STUDY ON SUBSURFACE FLOW UNDER AN ALTERNATE SANDBAR IN A RIVER BY NUMERICAL MODEL AND ITS APPLICATION TO THE KIZU RIVER

By

Abu Musa Md. Motaher Ahmed

Doctoral Student, Dept. of Civil Engineering, Nagoya University, Japan

Tetsuya Sumi

Assistant Professor, Dept. of Geo- & Environmental Engineering, Nagoya University, Japan

and

Tetsuro Tsujimoto

Professor, Dept. of Geo- & Environmental Engineering, Nagoya University, Japan

SYNOPSIS

Subsurface flow with alternate sandbars in a river for various topographic and hydraulic conditions is investigated by numerical simulation. A 2-D subsurface flow model based on the Dupuit-Forchheimer equation is used for subsurface flow computations. Surface water elevation at the edge of sandbar, which is measured in the laboratory experiment, provides the boundary conditions of the model. The 2-D subsurface flow model is verified by performing an experiment and applied to the field case. Subsurface flow patterns obtained by numerical simulations in the experimental and field scales are found to be similar. In addition, subsurface flow distribution patterns based on data measured in the Kizu river area and on simulated data agree reasonably well with the same surface flow conditions. Surface water elevation at the sandbar's edge also provided the boundary conditions for the subsurface flow model. In this paper, subsurface flow patterns and water budgets for various scenarios are analyzed and discussed with regard to exchange between surface and subsurface flow. The paper concludes with discussions on the effects of a secondary channel to the subsurface flow structures and on water budgets in the Kizu river area.

INTRODUCTION

In a natural stream with alternate sandbars, surface flow interacts with the subsurface flow in the riparian alternate sandbar when a hydraulic connection exists between the two different types of flow. River channelization work has often resulted in the formation of alternate sandbars and the stream shows meandering in its planform during low flow conditions. When the channel conveys low flow, subsurface flow becomes stronger, and its state depends on the surface water level in the channel. In the cases where surface flow contains pollutants and industrial wastes, alternate sandbars can then be a source for purification of surface water by exchanging them with subsurface water flowing in the sandbar. Moreover, backwater along sandbar and temporal ponds are important for the benthic community, and these water spaces are largely influenced by subsurface flow patterns. Subsurface flow distribution in the alternate sandbar in a meandering channel is important to estimate exchange flux between surface and subsurface water. Also ecologists and hydrologists have already noticed that local hydrologic interactions between surface water and groundwater play an important role in the stream ecosystem structure and function, Gibert *et al.* (7).

An understanding of surface-subsurface flow interaction on small scale requires a knowledge of subsurface flow paths and their linkage to streams, rates of exchange between surface water and subsurface water and the mechanisms that generate spatial and temporal variations in these processes. As reported by

Wroblicky *et al.* (16), the near stream interactions, for instance, interactions with alternate bar, have focused on stream geomorphic characteristics such as bed-form topography and its influence on hydrologic interchange and local groundwater systems.

Larkin and Sharp (12), Harvey *et al.* (10) and Wroblicky *et al.* (16) reported that the streams with meander bend generate lateral hyporheic zone where the exchange between surface and subsurface flow occurs under the surface water. The delineating characteristics of the hyporheic zone are the recharge of channel water to the subsurface in vertical and mixing with groundwater that has not yet reached the channel. Subsurface flow structures in the nearby aquifer influenced by the mountainous river are examined by Wroblicky *et al.* (16), Wondzell and Swampson(15). Harada *et al.* (9) studied the effects of interactions in the cases where small streams run in a highly permeable alluvial basin. Interactions between stream and alternate sandbar have been studied experimentally by Ahmed *et al.* (2) and the areas of potential interactions are known with respect to the spatial distribution of the surface water level in a stream and the subsurface water level in the riparian sandbar. They also discussed the subsurface flow structures influenced by surface flow structures for given channel flow conditions. Numerous explanations have been provided to explain the physical evidence of interactions between two separate flows (Cunningham and Sinclair (5), Ackerer *et al.* (1), Mitchell-Bruker & Haitjema (13)).

In this study, an investigation of subsurface flow patterns and water budget under an alternate sandbar in a river were carried out with various topographic and hydraulic conditions. Subsurface flow patterns and water budgets with these scenarios were also analyzed so as to discusses the exchange between surface and subsurface flow within the system. Subsurface flow pattern and water budget for a sandbar in the Kizu river under the conditions with and without a secondary channel on the sandbar are also investigated.

OBJECTIVES OF THE STUDY

The objectives of this study includes:

a) to determine spatial distributions of subsurface water levels relative to distributions of surface water elevations at the edge of sandbar for the given flow and bed conditions;
b) to delineate basic subsurface flow patterns that generate exchange between surface and subsurface flow;
c) to evaluate water budgets for the individual patterns and to compare them; and
d) to verify reliability of the subsurface flow model by applying it to the field

FLUME EXPERIMENT

Experiments were carried out to obtain boundary conditions for numerical simulation of subsurface water flow and also to complement a numerical simulation in order to clarify the relationships between subsurface flow patterns and surface flow conditions including bed shape.

Experimental set-up

A 600cm long and 50cm wide glass-sided horizontal flume is used for experiments. A pump circulated the steady-state discharge, and a stilling basin installed at the upstream position provided uniform flow at the entrance to the flume. A drainage basin is located at the downstream and a submersible pump is placed into it. The experimental set-up is shown in Fig.1. The surface water level at the downstream is adjusted by a tailgate, which also satisfied the periodic conditions in the channel. Well-graded sand with a median diameter of 2.1mm is used for the preparation of a model bed in the flume along with sandbar. The bed was moulded before each run and the sandbars are artificially created in the flume channel.

The bed elevation (z_b) is expressed by the Eq.1 as

$$z_b = D - (x - \frac{L}{2})I + a\sin\frac{2\pi(x - \frac{L}{2} + \frac{\lambda}{4})}{\lambda}\cos\frac{\pi y}{B} \qquad (1)$$

The average thickness of the permeable layer, D and sandbar wavelength, λ is taken as 15cm and 300cm, respectively. Here, L and B represent the length and width of the flume, respectively, I is the longitudinal slope of the flume bed and x and y are the co-ordinates. The amplitude, a of the sandbar is taken as an arbitrary value for the individual cases. The surface of the channel is fixed by uniform spray used for

wood varnishing to prevent sediment transport and disturbance to the permeability. This is verified by the column test for the permeability measurement. A digital point gauge is used to determine the channel bed and water surface elevation. Twenty piezometer tubes are installed at five lines at a 25cm intervals in x-direction and 5cm in y-direction as shown in Fig.1 to measure subsurface water elevations with respect to the impermeable layer.

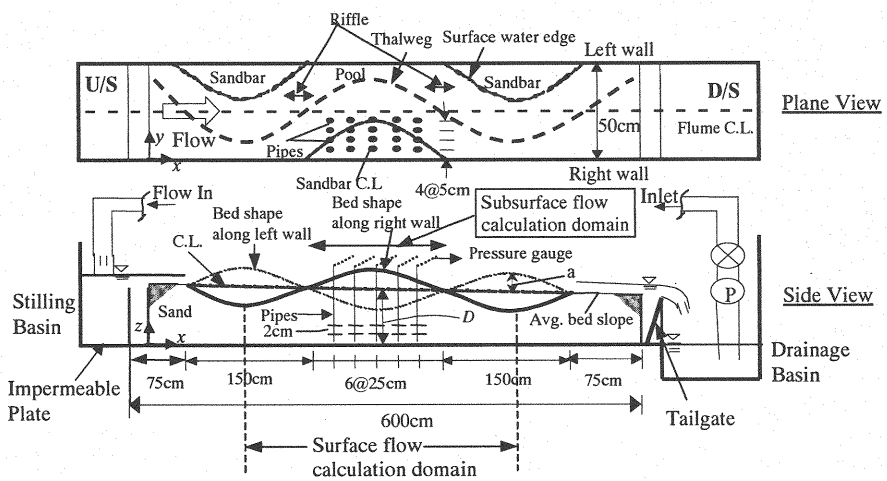

Fig.1 The experimental set-up

Experimental Runs

The sensitivity of the surface water profile to different amplitudes and bed slopes along the thalweg line for different surface flow discharges is studied keeping the B/D ratio the same in all cases. Subsurface water levels are measured by the piezometers installed into the sandbar. Spatial distributions of surface water levels along the edge of the sandbar with surface water are also recorded to use in the subsurface flow model as boundary conditions. The experimental conditions are shown in Table 1.

Table 1 Experimental conditions

Bed condition		Run No.		
Slope(I)	Amplitude a (cm)	Discharge, Q (cm^3/s)		
		1000	2000	3000
1/100	4.2	1a-1	1a-2	1a-3
	6.3	1b-1	1b-2	1b-3
	8.4	1c-1	1c-2	1c-3
1/200	4.2	2a-1	2a-2	2a-3
	6.3	2b-1	2b-2	2b-3
	8.4	2c-1	2c-2	2c-3

NUMERICAL SIMULATION OF SUBSURFACE FLOW

Numerical simulations are performed to simulate subsurface water levels with respect to impermeable layer within one sandbar for given boundary conditions and to estimate water budget quantities. In subsurface flow simulation, a steady state 2D depth averaged model is applied based on Dupuit's assumption that the impermeable layer is horizontal. It is also assumed that the boundary condition is the static surface water level along the sandbar's edge. Finite difference method with staggered grid is used for numerical solutions.

We assume the resistance to vertical flow is small compared to that of horizontal flow (Kirkham (11),

Strack (14)). The resistance due to a layer of fine sediments deposited at the stream-sandbar interface is assumed to be zero (Anderson and Woessner (3)). The capillary suction is negligible in comparison to the average subsurface water depth because the grain size used in the experiment is 2.1mm.

The simplified equation for steady two-dimensional unconfined horizontal flow with isotropic and uniform medium based on the Dupuit-Forchheimer assumption (Bouwer (4)) is used for conducting numerical simulation. The governing equation is

$$\frac{\partial}{\partial x}\left(kh\frac{\partial h}{\partial x}\right)+\frac{\partial}{\partial y}\left(kh\frac{\partial h}{\partial y}\right)=0 \qquad (2)$$

Eq.2 can be re-written in the simple form of Laplace equation as

$$\frac{k}{2}\left(\frac{\partial^2 h^2}{\partial x^2}+\frac{\partial^2 h^2}{\partial y^2}\right)=0 \qquad (3)$$

where h is subsurface water depth from horizontal impermeable layer; k is hydraulic conductivity of the permeable layer; and x and y are the coordinates in the longitudinal and transverse directions respectively.

Spatial distribution of subsurface water elevations is computed by solving Eq.3 after discretization. The boundary condition is the spatial distribution of surface water level, H at the interface between surface and subsurface water, which is obtained from the experiment for each run individually. A measured value of hydraulic conductivity (k=4.96 cm/s) of the same sand as used in the experiment has been considered to compute the subsurface flow flux as well as water budget under the sandbar. A definition sketch is shown in Fig.2, which provides the physical parameters necessary for numerical calculations.

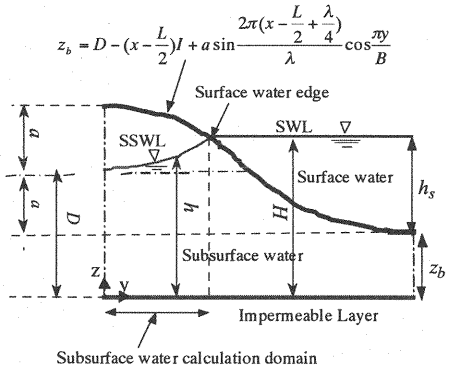

a - Amplitude of sandbar

D - Average thickness of the permeable layer

H - SWL from the Impermeable layer

h - SSWL from the Impermeable layer

z_b - Bed level from the impermeable layer

h_s - Surface water depth

SWL - Surface water level

SSWL - Subsurface water level

Fig.2 A typical cross-section showing surface/subsurface water interface with sandbar in a river

RESULTS AND DISCUSSION

The results of numerical simulations are shown as 2-dimensional distributions of subsurface water level and Darcy flux vector. The contour lines are compared in respect to variation in amplitude, discharge and average bed slope. Prior to making these comparisons, the 2-dimensional distributions of subsurface water level based on experiments and numerical simulations are compared with each other to verify the reliability of the subsurface flow model.

Spatial distributions of subsurface water level depend upon the distribution of surface water level. The bed level, z_b and corresponding surface water level, H with respect to impermeable layer measured along thalweg line for some cases are shown in Fig.3. This figure shows that for low flow the surface flow profiles at the immediate downstream of the riffle are steep, and that also the steepness of profiles are higher for higher amplitude and steep bed slope (case 1c-1). But the profile becomes milder with high discharge (case 1c-3). The surface water profile in the pool is almost horizontal for all cases. The effects of these profiles on the subsurface flow patterns are described later.

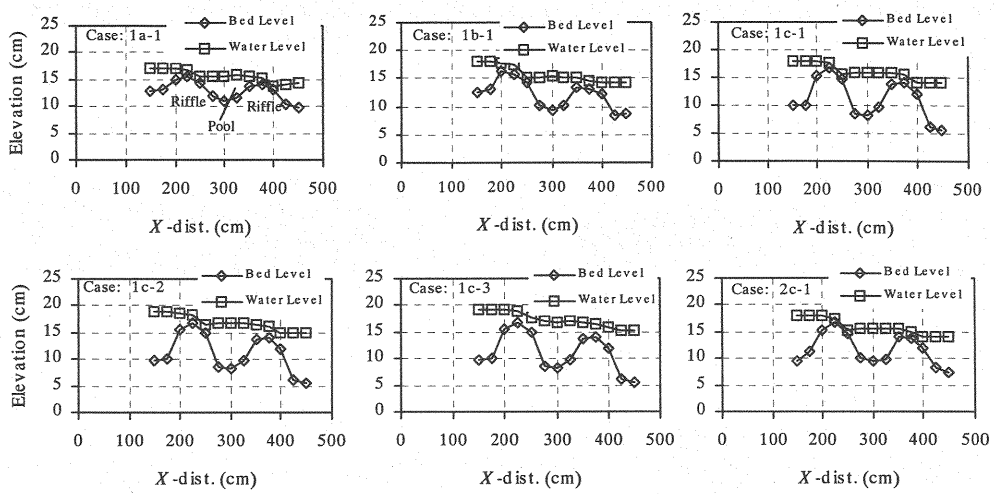

Fig.3 Surface water profile along thalweg line

The 2D distributions of subsurface water level in the sandbar based on the data measured in the experiment and calculated by numerical simulation for case 1c-1 is shown in Fig.4a and 4b, respectively. A comparison between these two figures shows that the 2D distributions of subsurface water level in the experiment and numerical simulation are identical. These two figures also indicate that 2D pattern of subsurface water flow at the upstream part is a diverging type and at the downstream part is a converging type.

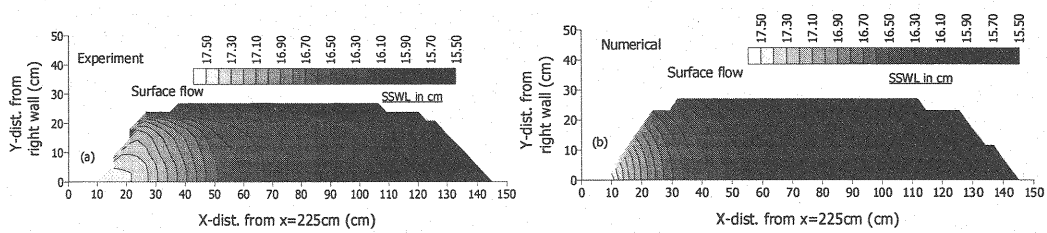

Fig.4 Subsurface water level distribution under the sandbar: comparison between experiment and numerical

Subsurface Flow Patterns based on numerical simulation

Subsurface flow patterns for different cases in numerical simulation are shown in Fig.5. This figure shows the comparison of subsurface flow patterns with respect to different amplitudes, discharge and bed slopes. By comparing the cases of different amplitudes, we can see that for lower amplitude (case 1a-1, Fig.5a) the subsurface flow contour lines are parallel at the upstream inflow part and that the spacing between the contour lines is relatively larger, which indicates a comparatively low inflow flux. This is due to the comparatively gentle slope of surface water (Fig.3) and gradual increase of sandbar's width towards the downstream direction. However, for medium amplitude (case 1b-1, Fig.5b), the contour lines are some what inclined at the surface water edge and the contour intervals are less than those for case 1a-1 which shows a higher inflow flux. This pattern is generated by the existence of moderate slope of the surface water (Fig.3). In cases of higher amplitude (case1c-1, Fig.5c), the contour lines are also inclined at the surface water edge and the spacing between the contour lines is smaller than those for cases 1a-1 and 1b-1, which show comparatively higher inflow flux. This is due to the steep surface water gradient, especially at the downstream of the riffle (case 1c-1, Fig.3). The downstream contour interval is larger for higher amplitude case (case 1c-1,

Fig.5c), which indicates low outflow flux at the downstream part of sandbar. On the other hand, the contour interval becomes smaller in the case of lower amplitude (case 1a-1, Fig.5a) and outflow flux is found to be higher.

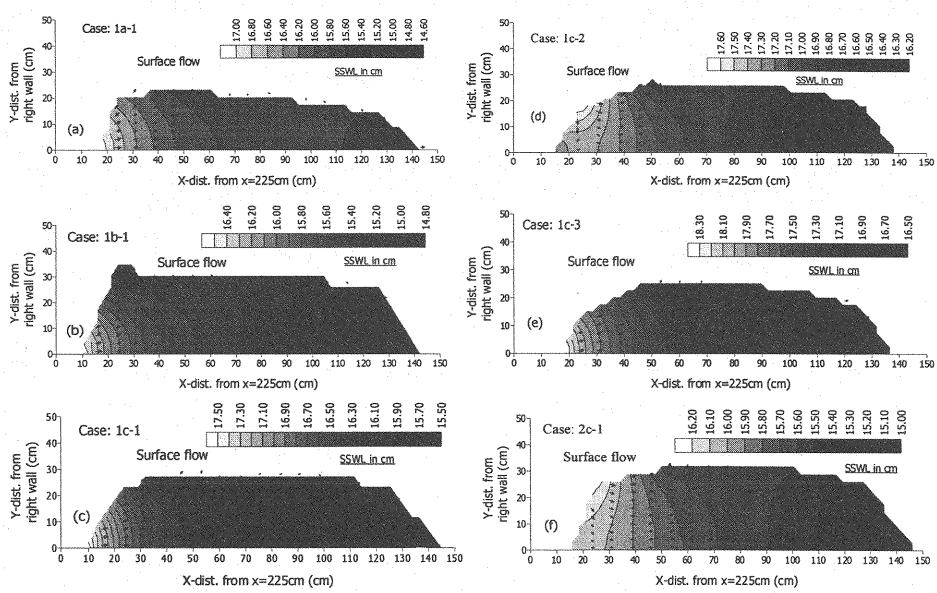

Fig.5 Subsurface flow patterns case-by-case

If we compare among the cases of different surface flow discharges with higher amplitude, we see that the spacing between the contour lines at the upstream part of sandbar increases with higher discharge (case 1c-3, Fig.5e) and this indicates lower inflow flux in comparison with the lower discharge case. On the other hand, the contour interval at the downstream part decreases with discharge. As a result, outflow flux becomes higher for higher discharge. This is due to the relatively mild gradient of surface water level.

If the bed slope cases are compared with each other, it can be seen that the contour intervals are smaller in steep bed slope cases (case 1c-1, Fig.5c) than those in mild slope cases (case 2c-1, Fig.5f) at the upstream part. This is due to same reason already described. The contour intervals at the downstream part are slightly larger in steep slope cases than those for mild slope cases. This is due to the effect of riffle and relative mound of sandbar at the downstream part (Fig.3).

The most evident tendency is that inflows near the upstream edge of sandbar contribute most of total inflow flux. However, inflow from pool occurs for higher discharge and lower amplitude cases.

Subsurface Water Budget

The possible exchange between surface water and subsurface water under alternate an sandbar in a river can be evaluated by the analysis of subsurface water budget along the surface water edge with sandbar. However, subsurface water budgets can be evaluated by plotting cross-sectional flux, Q_x' in x-direction. Q_x' can be expressed as,

$$Q_x'(x) = \int_{y=0}^{y=y_{end(x)}} \bar{q}_x(x,y)dy \qquad (4)$$

where $Q_x'(x)$ is the subsurface water flux along the cross-section at $x = x$; $y_{end(x)}$ is the transverse distance (at $x = x$) from right wall ($y = 0$) to surface water's edge; and $\bar{q}_x(x,y) = -kh(x,y)\dfrac{dh}{dx}$; where $\bar{q}_x(x,y)$ is the flux per unit width.

So, the discretized form of Eq.4 can be written as:

$$Q_x'(x) = \sum_{j=1}^{nj} k(h_i^2 - h_{i+1}^2)\frac{\Delta y}{2\Delta x} \qquad (5)$$

where h_i is the subsurface water level at *ith* node; h_{i+1} is the subsurface water level at *i+1th* node; Δx and Δy are the incremental distance in x and y directions respectively; $i = 1...ni$ is the *ith* node in x-axis and $j = 1...nj$ is the *jth* node in y-axis.

Q_x' along x-axis from upstream to downstream of a sandbar for a typical case is shown in Fig.6. The higher peak of Q_x' indicates a higher water exchange rate through the sandbar. This figure shows that at the upstream part of the sandbar, Q_x' is higher at a certain distance downward from the upstream end. At the downstream part, Q_x' is higher at a section where the sandbar's edge line turns towards the downstream end of the sandbar with wall but the magnitude is very low compared to the upstream part.

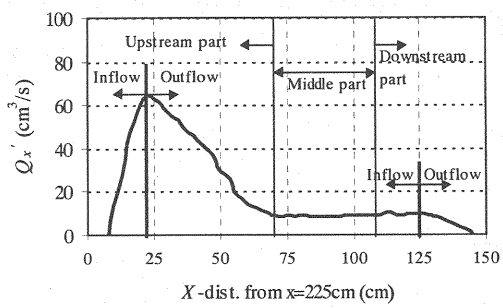

Fig.6 Q_x' in longitudinal direction (case 1c-1)

The inflow and outflow boundary flux at the upstream and downstream part of sandbar is shown in Table 2. Surface water inflows near the upstream end of sandbar account for most of total inflow flux. If we compare the budget for different amplitudes with low discharge (case 1a-1, 1b-1 and 1c-1), we see that the higher amplitude (case 1c-1) produces higher inflow and outflow fluxes than that of lower amplitude and longitudinal flow is dominant under this bed shape. But at the downstream part, inflow from pool occurs in lower amplitude case and this is the only source of outflow flux, which is greater than that of higher amplitude case. Infact, no inflow occurs from the pool to subsurface water in higher amplitude case. The medium amplitude conveys longitudinal flow from the upstream and inflow also occurs from the pool at the downstream. As a result, outflow flux is higher in comparison to the other cases.

Table 2 Inflow and outflow boundary flux

Case	Channel flow discharge (cm^3/s)	Upstream part of sandbar		Downstream part of sandbar		Total flux (inflow/outflow) (cm^3/s)
		Inflow flux (cm^3/s)	Outflow flux (cm^3/s)	Inflow flux (cm^3/s)	Outflow flux (cm^3/s)	
1a-1	1000	50	50	12	12	62
1b-1	1000	62	52	8	18	70
1c-1	1000	70	60	0	10	70
1c-2	2000	50	42	11	19	61
1c-3	3000	45	40	17	22	62
2c-1	1000	40	32	8	16	48

A comparison of the discharges (case 1c-1, 1c-2 and 1c-3) show that at the upstream part, inflow and outflow fluxes are higher for lower discharge and also longitudinal flow is dominant. At the downstream part, inflow from pool is higher for higher discharge, and the outflow flux becomes higher due to a higher inflow flux from pool and residual flux from the upstream. If we compare budget expressions in different bed slopes, we see inflow and outflow fluxes at the upstream part are much higher in the case of steep slope (case 1c-1) than that in the case of mild slope (case 2c-1) and also the dominance of longitudinal flow is stronger in steep slope case. At the downstream part, inflow from the pool occurs only in mild slope, which increases the outflow flux. It is observed that lower amplitude or higher discharge enhances lateral inflow from the pool and that the outflow flux at the downstream part is higher.

Table 2 illustrates that a steep slope and higher amplitude with lower discharge causes higher inflow and outflow flux at the upstream part of sandbar. On the other hand, lower amplitude and higher discharge brings about higher inflow and outflow flux at the downstream part. Inflow from pool occurs due to higher gradient of surface water near the downstream part and the effect of downstream riffle. At the upstream part, the evident characteristic is that most of the flow coming from upstream side goes out to the pool due to riffle. The steep gradient of riffle makes the interval between the subsurface water level contours smaller and, as a result, subsurface water's gradient is steep, which shows a strong diverging trend here.

FIELD APPLICATION OF THE SUBSURFACE FLOW MODEL

Subsurface flow model as developed on the basis of experimental data is applied to the field problem and data measured in the Kizu river area is used for the simulation. The purpose is to compare the simulated results with measured field data, and to discuss the difference of subsurface flow patterns due to different surface flow conditions.

Field Data Collection and Analysis

(a) Study site

The study includes one alternate sandbar in the Kizu river area, length and maximum width of which are about 900m and 350m, respectively. The river tends to meander in its planform around the study reach as shown in Fig.7. The main characteristics of the site that was investigated were obtained by material sample measurements and core samplings in the filed and are presented in Table 3.

The average annual maximum flow is 1800 m^3/s and the minimum flow recorded in 1999 is 5.7 m^3/s. A drainage channel is located at the reverse side of the main channel and the water level of this channel is very low. This channel drains out water into the main channel at the downstream of the sandbar. It should be mentioned that a secondary channel started to develop across the sandbar, which became evident in April 2000. Initially, the secondary channel was attracted by partial channel flow in the flood season and the channel completely dried up in the winter season. However, now the secondary channel conveys a part of channel flow in all seasons. It can be predicted by the field measurement and by numerical simulation that the influence of secondary channel plays an important role in changing subsurface flow patterns in the alternate sandbar.

Table 3 Main characteristics of the study area

Watershed characteristics	Values
Average bed gradient (I)	1150
Max. channel width (B), m	400
Max. width of sandbar, m	350
Max. channel width/bar wavelength ratio (B/λ)	1:6
*Median bed sediment diameter (D_{50}), m	0.0001-0.03
**Average hydraulic conductivity (k), m/s	0.0002
Average thickness of permeable layer (D), m	15

Source: *Egashira (6), ** Harada (8)

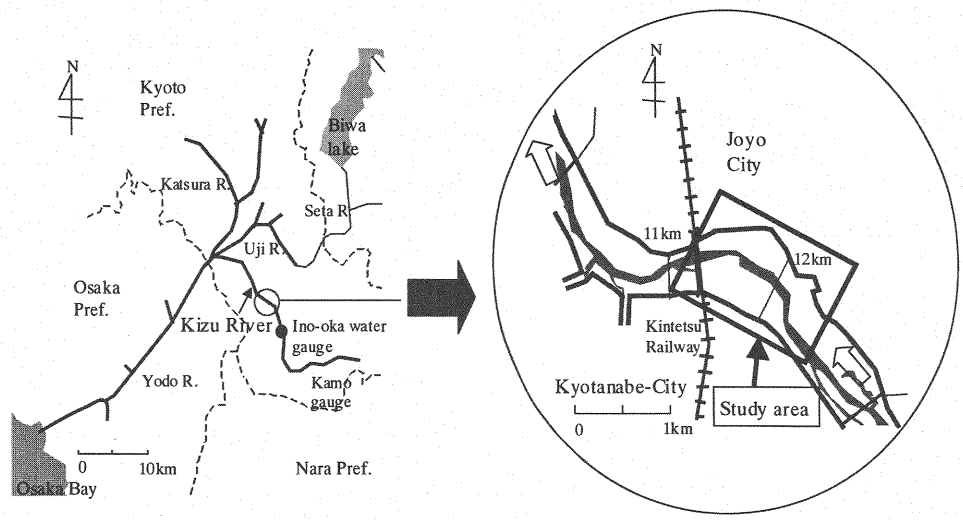

Fig.7 The Kizu river showing study area

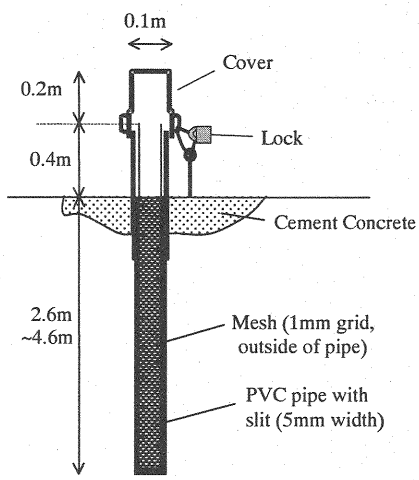

Fig.8 Piezometric well

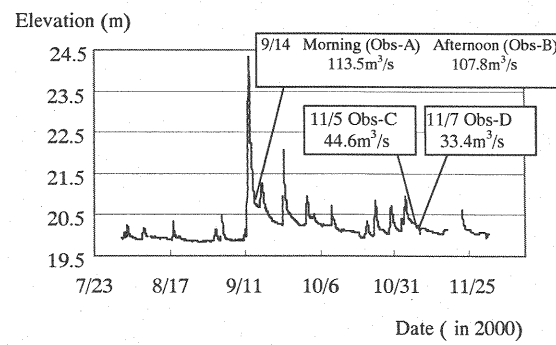

Fig.9 Surface water elevation measured at Ino-oka gauge with some known discharge

(b) Instrumentation and field data

Several wells were installed on the sandbar near the main channel at random as shown in Fig.10 to measure subsurface water levels (piezometric head). The arrangement of the piezometric well is shown in Fig.8. Also, surface water levels at the edge with sandbar are measured by the staff gauges. The same technique is applied in measuring surface water levels in the secondary and drainage channel. Surface water levels are used as boundary conditions for 2D subsurface flow model. Surface water elevation is recorded at Ino-oka gauging station upstream of the site studied in order to obtain surface water discharge from *H-Q* relationships. Surface water elevation recorded on different dates in the year 2000, for those *H-Q* relationships are known, is shown in Fig.9. This figure also shows the gauge levels against corresponding discharge measured at different observation period (Obs-A, B, C and D). These four cases include secondary channel. Obs-A and B corresponds to the cases of unsteady flow with sharp recession whereas Obs-C and D are the cases of unsteady flow, but with a slow recession period. On the other hand, Obs-E is a low flow case without secondary channel under the steady condition.

Subsurface Flow Patterns

(a) Based on observed data

2D distribution of subsurface water level based on measured data in a sandbar along the Kizu River during two low flow cases correspond to late recession period (Obs-E and Obs-D) are shown in Fig.10a and 10b, respectively. These figures show the subsurface flow patterns without and with the secondary channel. From the comparisons between Fig.5c and Fig.10a, it is evident that although the scales are different, the flow patterns in a sandbar without secondary channel (Obs-E) show a similar pattern so one found in the numerical simulations in experimental scale.

(b) Based on numerical simulation

The subsurface flow model used in the experimental scale is applied to field case. Surface water levels measured at the sandbar's edge are used as boundary conditions of the model. The boundary condition's data are interpolated by the simple interpolation technique to obtain data at non-measured points. The 2D distribution of subsurface water levels obtained by numerical simulations for Obs- E and D are shown in Fig.11a and Fig.11b, respectively. If we compare between Fig.10a and 11a or between Fig.10b and 11b, we can see a similarity in flow patterns between the observed and the numerical simulation. From these comparisons, it is clear that the 2D subsurface flow model is adequate to predict the fundamental flow patterns in any surface flow conditions. The flow patterns and water budgets under the condition without and with secondary channel are discussed later.

COMPARISON BETWEEN THE CONDITIONS WITH AND WITHOUT SECONDARY CHANNEL BASED ON NUMERICAL RESULTS

Subsurface Flow Patterns

At the upstream part of sandbar, the contour interval is smaller under the condition with secondary channel than without secondary channel. Under the condition with secondary channel, flow in secondary channel contributes extra flux laterally in both part (part A and B, Fig 10b or 11b) of the sandbar. In secondary channel, the surface water gradient is changed gradually and water level is higher than in the main channel. The inflow flux contributed by secondary channel in part B partially goes to the drainage channel because of the low water level exists in the drainage channel. The rest of the flux in part B and the total flux in part A flow in a downstream direction before going to the main channel.

At the downstream part, under the condition without secondary channel, drainage channel has a significant influence where we can see that some of the contour lines are almost parallel longitudinally. This means that strong lateral outflow to drainage channel occurs in the middle reach.

Under the condition with secondary channel, inflow or outflow flux is governed by both secondary and drainage channels. However, the effect at the upstream part governed only by secondary channel show a similar trend but is rather weaker than under the condition without secondary channel due to the flux from secondary channel. But the outflow characteristics at the downstream are opposite and outflow is stronger under the condition with secondary channel than under the condition without secondary channel.

The flow patterns and their trend without and with the existence of secondary channel are schematically shown in Fig.12 and 13, respectively. Figure 12 indicates that at the upstream part of the sandbar the flow pattern shows diverging trend and at the downstream part it shows horizontal trend with little outflow towards drainage channel. But Fig.13 shows strong transverse flow at the upstream part and strong longitudinal flow at the downstream part in part A. The secondary channel changed the whole flow pattern where downstream part of part B is subject to higher transverse flow towards drainage channel due to higher difference of water level between the two channels. Under the condition with secondary channel, these flow patterns are predicted because the surface water level difference between the secondary channel and the main channel is high at the upstream part, which is produced by the riffle at the upstream side.

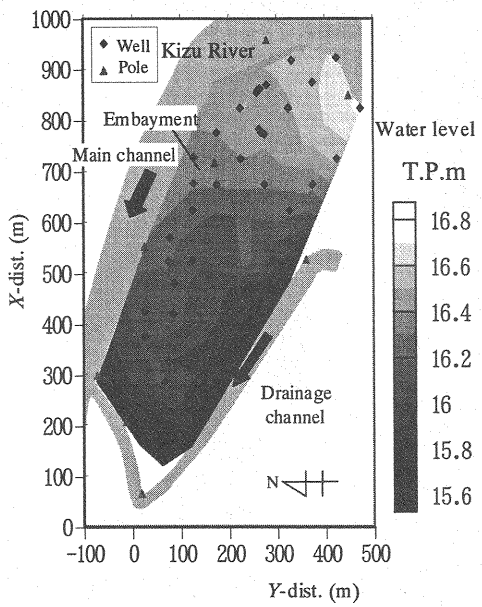

Fig.10a Distribution of subsurface water level at Obs-E (Observed on 1999/6/5)

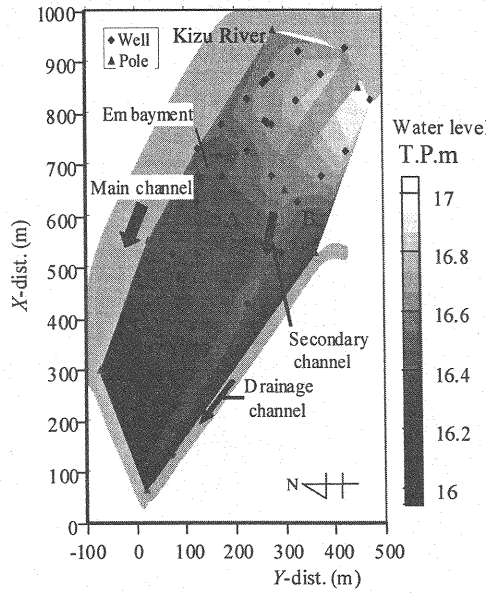

Fig.10b Distribution of subsurface water level at Obs-D (Observed on 2000/11/7)

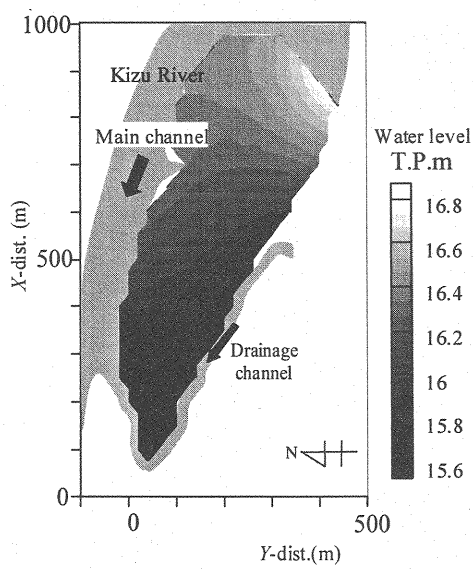

Fig.11a Distribution of subsurface water level at Obs-E (Numerical simulation)

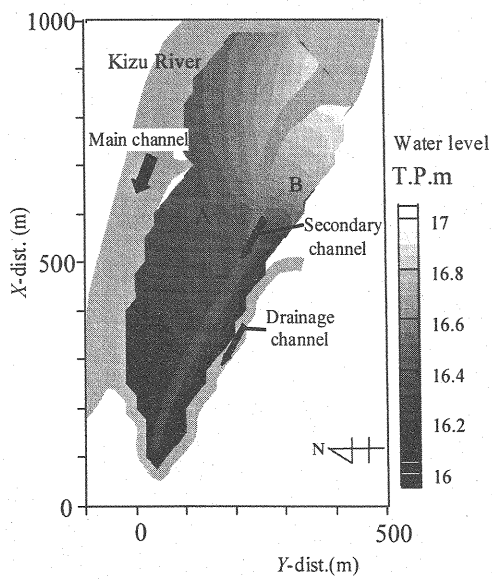

Fig.11b Distribution of subsurface water level at Obs-D (Numerical simulation)

But in both cases, the surface water level difference between secondary channel and main channel is small at the downstream part and flow rate is relatively low. A comparison between figures 12 and 13 reveals that the secondary channel has a significant influence on the upstream part of the sandbar, which weakens the diverging trend and decelerates the flow rates longitudinally and accelerates laterally.

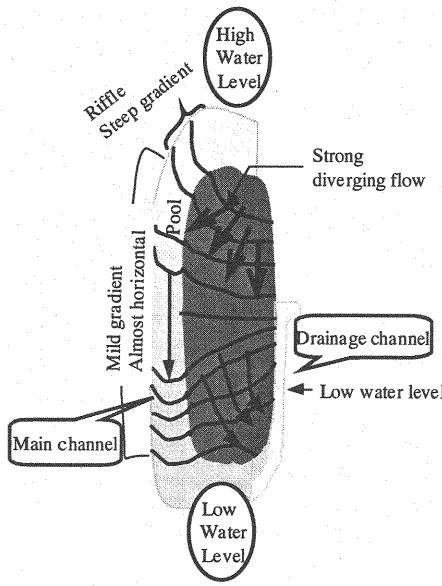

Fig.12 Schematic diagram of subsurface flow patterns without secondary channel

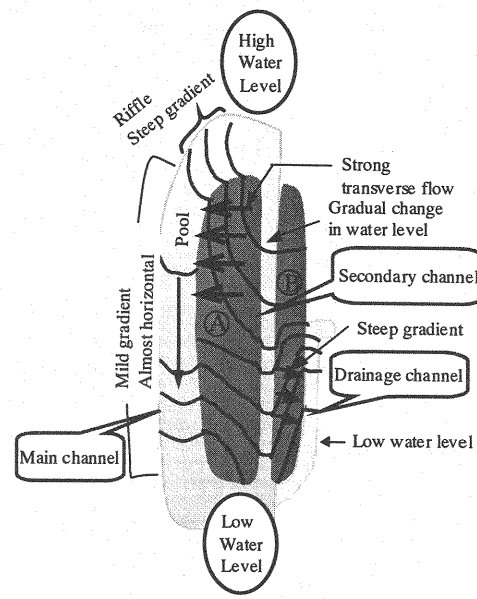

Fig.13 Schematic diagram of subsurface flow patterns with secondary channel

Subsurface Water Budget

The total subsurface water budget over the whole sandbar is calculated by using the same technique used in the experimental scale. The total budget or volumetric flow rate through the whole sandbar is shown in Table 4.

Table 4 Total flow rate

Observation case	Date	Channel flow discharge, m^3/s	Subsurface Flow rate, m^3/day(Part A)	Subsurface Flow rate, m^3/day(Part B)	Total Flow Rate (m^3/day)
A	2000/9/14 (AM)	113.5	585	1366	1951
B	2000/9/14 (PM)	107.8	593	1350	1944
C	2000/11/5	44.6	226	792	1019
D	2000/11/7	33.4	269	541	810
E	1999/6/5	34.4	-	-	366

Table 4 shows that total subsurface flow rate is higher for higher discharge provided that the topographic and hydraulic conditions are different. In the cases with secondary channel (Obs-A, B, C and D), the flow rate is higher in part B than part A due to the higher gradient between secondary channel and drainage channel. Part A is dominated by the resultant flux effects from the main channel and the secondary channel and part B only by the effects from secondary channel. In secondary channel, changes in water level with discharge are relatively small in comparison to that in the main channel. If we compare cases D and E, we can see that for the same channel discharge, the total flux is higher under the condition with secondary channel. The higher quantity is due to the flux effect of secondary channel.

Differences between Obs-A and B, and between C and D is small due to the similarity of surface water's conditions. On the other hand, water budget in Obs-A and -B corresponds to high discharge is higher than those in Obs-C and -D at both parts (part A and B). Surface water's shape is more or less the same with a slight difference of absolute elevation due to different discharges. But in the cases of Obs-A and –B, water

levels at the upstream part of secondary channel relative to the main channel is higher than in the cases of Obs-C and -D. The difference in the surface water's conditions results in producing a higher subsurface flux from the secondary channel towards main channel or drainage channel in cases of higher discharges.

CONCLUSIONS

Subsurface flow pattern and water budget under the alternate sandbar for various surface flow scenarios with different bed shapes is understood by numerical simulation. This study concludes that surface water profile and bed shape greatly affects the subsurface flow pattern and water budget. The subsurface flow pattern at the upstream part of sandbar shows diverging trend and this trend is stronger in lower discharge case on steep bed slope with higher amplitude. The similar findings are obtained by water budget analysis. This trend is due to the higher gradient of surface water on the riffle formed by this bed shape. The subsurface flow patterns and water budgets show that at the downstream part, inflow from pool occurs in some cases, which generates converging trend but the trend is stronger for higher discharge case on steep bed with lower amplitude. This trend is due to the effects of the riffle on surface water level at its (riffle) upstream. The pool and riffle sequences create a steep gradient at the surface water level on the riffle and almost no gradient in the pool. Due to low gradient in the pool, no transverse exchange was observed in the middle part of sandbar and as such subsurface flow is nearly horizontal. The flow pattern and water budget shows that the 2-D characteristics are stronger at the upstream part of the sandbar than that at the downstream part.

Agreements between the numerical simulation and experiment, and also, between the numerical and the field were found to be reasonably satisfactory. A comparison of flow pattern and water budget between the conditions with and without secondary channel reveal that the secondary channel on the sandbar accelerates lateral exchange of flow and decelerates the flow rate in longitudinal direction. The secondary channel changes the strong diverging flow to transverse flow at the upstream part of sandbar. The findings of this study show clearly that the surface water's property as the boundary conditions plays an important role on subsurface flow. Hence the studies under various surface water properties provided by the bed shapes are needed in the future.

REFERENCES

1. Ackerer, Ph., Esteves, M and R. Kohane : Modelling interaction between groundwater and surface water: a case study in computational methods in subsurface hydrology, Proc. 8th Int. Conf. Comp. Methods Water Resour., Springer-Verlag, Berlin, pp. 69-75, 1990.
2. Ahmed, A.M.M.M., T. Sumi and T. Tsujimoto : Subsurface flow in a stream with alternate sandbars, Annual J. of Hydraulic Engg., Japan Soc. Civ. Engineers, Vol. 45, pp. 349-355, 2000.
3. Anderson, M.P. and W.W. Woessner : Applied groundwater modelling: simulation of flow and advective transport, Academic, San Diego, Calif, 1992.
4. Bouwer, H.: Groundwater Hydrology, McGraw-Hill, Newyork, 1978.
5. Cunningham, A.B. and P.J. Sinclair : Application and analysis of a coupled surface and groundwater model, J. of Hydrol, 43, pp.129-148, 1979.
6. Egashira, S. : Report on the grain size distribution data of the Kizu river, Memo Ritsumeikan University, Kyoto, Japan, 1998 (In Japanese).
7. Gibert, J., D. L. Danielopol and J.A. Stanford : Groundwater Ecology, 571 pp., Academic, San Diego, Calif, 1994.
8. Harada, M. : Substrate structure and subsurface flow in the River Kizu, Annual Report, River Ecology Research Group of Japan, Ministry of Construction, Japan, 2001 (In Japanese).
9. Harada, M., Y. Tsuge and M.A. Marino : Effects of interaction between stream and aquifer on stream condition in alluvial basin, IAHS Int. Symp. on Int. Water Res. Management, UC Davis, 2000.
10. Harvey, J.W., Wagner, B.J. and K.E. Bencala : Evaluating the reliability of the stream tracer approach to characterize stream-subsurface water exchange, Water Resources Research, 32(8), pp.2441-2451, 1996.
11. Kirkham, D. : Explanation of Paradoxes in Dupuit-Forcheimer Seepage Theory, Water Resour. Res., 3(2), pp.609-622, 1967.
12. Larkin, R.J. and J.M. Sharp : On the relationship between river basin geomorphology, aquifer hydraulics, and ground-water flow direction in alluvial aquifers, Geol. Soc. Am. Bull., 104, pp.1608-1620, 1992.
13. Mitchell-Bruker, S. and H.M. Haitjema : Modelling steady state conjunctive groundwater and surface water flow with analytical elements, Water Resour. Res., 32(9), pp.2725-2732, 1996.

14. Strack, O.D.L. : Three-dimensional streamlines in Dupuit-Forchheimer Models, Water Resour. Res., 22(8), pp.1263-1272, 1984.
15. Wondzell, S.M. and F.J. Swanson : Seasonal and storm dynamics of the hyporheic zone of a 4th-order mountain stream. I: Hydrological processes, J. of North American Benthological Society, 15(1), pp.3-19, 1996.
16. Wroblicky, G.J., Campana, M.E., Valett, H.M. and C.N. Dahm : Seasonal variation in surface-subsurface water exchange and lateral hyporheic area of two stream-aquifer systems, Water Resources Research, 34 (3), pp.317-328, 1998.

APPENDIX – NOTATION

The following symbols are used in this paper:

a	= amplitude of the sandbar;
B	= width of the flume;
D	= average thickness of the permeable layer;
D_{50}	=Median bed sediment diameter;
h	= subsurface water depth from impermeable layer;
H	= surface water depth from impermeable layer;
z_b	= bed level with respect to impermeable layer;
h_s	= surface water depth;
I	= longitudinal slope of the flume bed;
k	= hydraulic conductivity of the permeable layer;
L	= length of the flume;
$Q_x'(x)$	= residual subsurface water flux;
$\overline{q}_x(x, y)$	= flux in x-direction per unit width as a function of y
SWL	= surface water level;
SSWL	= subsurface water level;
x, y	= coordinates; and
λ	= wavelength of sandbar.

(Received August 20, 2001 ; revised February 22, 2002)